Comparison of MUSIC, Unitary ESPRIT, and SAGE Algorithms for Estimating 3D Angles in Wireless Channels

Rui Feng[1], Yu Liu[1], Jie Huang[1], Jian Sun[1,2], and Cheng-Xiang Wang[3]
[1]Shandong Provincial Key Lab of Wireless Communication Technologies, Shandong University, Jinan, Shandong, 250100, China.
[2]State Key Lab. of Millimeter Waves, Southeast University, Nanjing, 210096, China.
[3]Institute of Sensors, Signals and Systems, School of Engineering & Physical Sciences, Heriot-Watt University, Edinburgh, EH14 4AS, U.K.
Email: fengxiurui604@163.com, xinwenliuyu@163.com, hj_1204@sina.cn, sunjian@sdu.edu.cn, cheng-xiang.wang@hw.ac.uk

***Abstract*—Joint estimation of azimuth and elevation angles is of great importance in source localization and channel characterization. Firstly, some basic knowledge of three typical parametric estimation algorithms are introduced in this paper, i.e., multiple signal classification (MUSIC), Unitary estimation of signal parameter via rotational invariance technique (ESPRIT), and space-alternating generalized expectation-maximization (SAGE) algorithms. Each algorithm is capable of extracting both azimuth angle of arrival (AAoA) and elevation angle of arrival (EAoA) of multi-paths jointly. It is pointed out that the SAGE and MUSIC algorithms have higher complexity than the Unitary ESPRIT algorithm due to the iteration/angle searching procedure. Secondly, impacts of antenna number, closely spaced paths, and signal-to-noise ratio (SNR) on estimation performance of three algorithms are analyzed. Results show that the Unitary ESPRIT algorithm has lower accuracy in comparison with the MUSIC and SAGE algorithms when antenna number and SNR are large. Finally, three algorithms are applied to estimate multipath parameters in 16 GHz massive MIMO channel measurements. It is shown that the Unitary ESPRIT algorithm performs less satisfactory in MPCs extraction, while MUSIC can provide comparable results with the SAGE algorithm.**

***Index Terms*—MUSIC, Unitary ESPRIT, SAGE algorithm, massive MIMO, angle of arrival (AoA).**

I. Introduction

In wireless communications, signals emitted from the transmitter (Tx) arrive at the receiver (Rx) through multipaths, which are generated by reflection, diffraction, and scattering. Multipath components (MPCs) have different complex amplitudes, delays, AAoAs, and EAoAs. To have a better understanding of wireless channels in the fifth generation (5G) systems using, e.g., millimeter wave (mmWave) and massive multiple-input multiple output (MIMO) technologies [1], directional characteristics are widely studied to benefit the source location, channel modeling, etc.

There are mainly three classical categories of array signal processing methods can be used to estimate directional information, namely spectral-based method, parametric subspace-based estimation technique, and deterministic parametric estimation [2], [3]. The first kind of methods can be further classified into beamforming and subspace-based methods, in which Bartlett beamforming and MUSIC algorithms are two representative methods, respectively. They estimate AoAs by searching for the angles that corresponding to the multiple local maxima of the pseudo spectrum [4]. It was pointed in [3] that the MUSIC method can provide statistically consistent estimates in contrast to the beamforming method. The ESPRIT algorithm is within the second kind of algorithm [5], [6]. It employs the invariance property of two displacement arrays and calculate the AoA directly, thus, to offer lower complexity than the spectral-based method. However, the accuracy of ESPRIT algorithm is lower than that of MUSIC algorithm. Unitary ESPRIT algorithm was latter proposed to further reduce the computational burden of ESPRIT algorithm by transforming the calculation into real-valued space and improve the estimation accuracy [7]. Within the third category are the expectation-maximization (EM) and SAGE algorithms. They are able to estimate delay, AoA, angle of departure (AoD), and complex amplitude jointly [8]. This kind of methods have high accuracy, but also very high complexity due to the iteration procedure. The SAGE algorithm is an extension of the EM algorithm and divides the estimated parameters into several subsets in the maximization (M) step [2].

In real time signal processing, the complexity and accuracy of parameter estimation algorithms should both be considered. Many researchers resort to MUSIC, ESPRIT, and the improvements of them to extract directional information. In [10], MUSIC and SAGE algorithms were used to study the impacts of horn antenna's half-power beamwidth and stepping strategy on root mean square error (RMSE). It was demonstrated that the MUSIC algorithm can provide similar results to the SAGE algorithm, yet with significantly reduced time consumption. In [11], Unitary ESPRIT algorithm was used to jointly estimate AAoA and EAoA for massive MIMO system with different antenna configuration and source number. It was indicated that the Unitary ESPRIT algorithm works well in massive MIMO channels.

However, there is the lack of literature regarding the comparison of these three algorithms in both synthetic and real channel parameter estimations. To fill this gap, the pros and cons of the MUSIC, Unitary ESPRIT, and SAGE algorithms are compared using Monte Carlo simulations. The parameter

978-1-5386-4502-4/17/$31.00 ©2017 IEEE

estimation results of the massive MIMO channel measurement data at 16 GHz are compared using the MUSIC, Unitary ESPRIT, and SAGE algorithm.

The remainder of this paper is organized as follows. The signal model is introduced in Section II. Basic concepts of MUSIC, Unitary ESPRIT, and SAGE algorithms are introduced in Section III. In Section IV, estimation performances are analyzed in synthetic environment and data processing results are compared in real massive MIMO channel environment. Finally, conclusions are drawn in Section V.

II. Signal Model

In a narrowband far-field wireless communication scenario, the output at the Rx array contributed by the l-th multipath can be expressed as

$$\mathbf{X}_l(t) = \mathbf{c}(u_l, v_l)s_l(t) + n_l(t) \tag{1}$$

where $\mathbf{c}(u_l, v_l)$, $s_l(t)$, and $n_l(t)$ are the steering vector, transmitted signal, and complex white Gaussian noise, respectively. Considering a $M = M_1 \times M_2$ horizontal uniform rectangular array (URA) lying in the x-y plane, the antenna index can be written as (m_1, m_2) with $1 \le m_1 \le M_1$ and $1 \le m_2 \le M_2$. Then, the antenna response of the (m_1, m_2)-th antenna to a wave impinging from a certain direction can be represented as

$$c_{m_1,m_2}(u_l, v_l) = \exp\left\{-j[(m_1-1)u_l + (m_2-1)v_l]\right\}. \tag{2}$$

The phase shifts caused by antenna displacements in x and y directions, namely u_l and v_l, can be written as

$$u_l = 2\pi\lambda^{-1}d_x cos\phi_l sin\theta_l \tag{3}$$

$$v_l = 2\pi\lambda^{-1}d_y sin\phi_l sin\theta_l \tag{4}$$

where λ, ϕ_l, and θ_l denote the wavelength, AAoA, and EAoA. The equidistance between two adjacent antennas is d_x in the x-direction and d_y in the y-direction, respectively. It is usually assumed equal to or less than half of the wavelength, thus, to have a one-to-one map between the antenna response and arrival direction.

For the convenience of the following analysis, we write $\mathbf{c}(u_l, v_l)$ in the following form,

$$\mathbf{c}(u_l, v_l) = \mathbf{c}(u_l) \otimes \mathbf{c}(v_l), 1 \le l \le L \tag{5}$$

where

$$\mathbf{c}(u_l) = [1, e^{-ju_l}, ..., e^{-j(M_1-1)u_l}]^{\mathrm{T}} \tag{6}$$

and

$$\mathbf{c}(v_l) = [1, e^{-jv_l}, ..., e^{-j(M_2-1)v_l}]^{\mathrm{T}} \tag{7}$$

with $\otimes$ and $[\cdot]^{\mathrm{T}}$ denote the Kronecker product and transpose operator, respectively. That means we stretch the steering vector into a $(M_1 \times M_2) \times 1$ column vector.

Further considering K-point sampled output signal,

$$\mathbf{X}_l(k) = \mathbf{c}(u_l, v_l)s_l(k) + n_l(k), 1 \le k \le K \tag{8}$$

the total output signal at the Rx can be expressed by summing L multipaths up, i.e.,

$$\mathbf{Y}(k) = \sum_{l=1}^{L} \mathbf{X}_l(k) = \mathbf{C}\mathbf{S}(k) + \mathbf{N}(k) \tag{9}$$

where $\mathbf{C} = [\mathbf{c}(u_1, v_1), ..., \mathbf{c}(u_L, v_L)]$, $\mathbf{S}(k) = [\mathbf{s}_1(k), ..., \mathbf{s}_L(k)]^{\mathrm{T}}$, and $\mathbf{N}(k) = [\mathbf{n}_1(k), ..., \mathbf{n}_L(k)]^{\mathrm{T}}$.

As MUSIC and Unitary ESPRIT algorithms are both based on the spatial covariance matrix to estimate the AoAs of MPCs, here we give it as

$$\begin{aligned} \mathbf{R} &= \frac{1}{K}\sum_{k=1}^{K} \mathbf{Y}(k)\mathbf{Y}^{\mathrm{H}}(k) \\ &= \mathbf{C}\mathrm{E}\left\{\mathbf{S}(k)\mathbf{S}^{\mathrm{H}}(k)\right\}\mathbf{C}^{\mathrm{H}} + \mathrm{E}\left\{\mathbf{N}(k)\mathbf{N}^{\mathrm{H}}(k)\right\} \\ &= \mathbf{C}\mathbf{P}\mathbf{C}^{\mathrm{H}} + E\left\{\mathbf{N}(k)\mathbf{N}^{\mathrm{H}}(k)\right\}. \end{aligned} \tag{10}$$

where $[\cdot]^{\mathrm{H}}$ denotes the Hermitian operator and $\mathbf{P}$ is the source covariance matrix.

In (10), the impinging signals and noises are assumed to be uncorrelated. If the signals are also uncorrelated and $L < M$, the rank of the source covariance matrix $r(\mathbf{P}) = L$. Therefore, $r(\mathbf{C}\mathbf{P}\mathbf{C}^{\mathrm{H}}) = L < M$, that means

$$\left|\mathbf{C}\mathbf{P}\mathbf{C}^{\mathrm{H}}\right| = |\mathbf{R} - \gamma\mathbf{R}_{\mathbf{0}}| = 0 \tag{11}$$

where γ can only be the $(M-L)$ minimum eigenvalues. Thus, $\mathbf{R}$ can be separated into two parts,

$$\mathbf{R} = \mathbf{E}_s\mathbf{\Lambda}_s\mathbf{E}_s^{\mathrm{H}} + \mathbf{E}_n\mathbf{\Lambda}_n\mathbf{E}_n^{\mathrm{H}} \tag{12}$$

with eigenvectors $\mathbf{E}_s$ correspond to the L larger eigenvalues $\gamma_s = diag\{\gamma_1, ..., \gamma_L\}$ form the signal subspace, and eigenvectors $\mathbf{E}_n$ correspond to the $M - L$ smaller eigenvalues $\gamma_n = diag\{\gamma_{L+1}, ..., \gamma_M\}$ form the noise subspace.

III. Basic Concepts of MUSIC, Unitary ESPRIT, and SAGE Algorithms

A. MUSIC Algorithm

Considering that the noise subspace is orthogonal to the signals theoretically, i.e.,

$$\mathbf{E}_n^{\mathrm{H}}\mathbf{C} = 0 \tag{13}$$

the direction finding problem can be transferred to calculate the Euclidian distance between $\mathbf{E}_n^{\mathrm{H}}$ and $\mathbf{C}$ in practical, and find the AoAs that can minimize the distance. Thus, MUSIC spatial spectrum is defined as the inverse of the Euclidian distance [4], i.e.,

$$P_{MUSIC} = \frac{\mathbf{C}^{\mathrm{H}}\mathbf{C}}{\mathbf{C}^{\mathrm{H}}\mathbf{E}_n\mathbf{E}_n^{\mathrm{H}}\mathbf{C}}. \tag{14}$$

Note that it is not a true spectrum in any sense. AAoAs and EAoAs can be found by searching the angles that are corresponding to the spatial spectrum peaks.

B. Unitary ESPRIT Algorithm

Unitary ESPRIT algorithm transforms the complex-valued calculation of the ESPRIT algorithm into real-valued to reduce the complexity. It employs the centrosymmetric property of the Rx array, i.e., when M_1 and M_2 are odd, (6) and (7) can be re-written as

$$\mathbf{c}(u_l) = [e^{-j(\frac{M_1-1}{2})u_l}, ..., e^{-ju_l}, 1, e^{ju_l}, ..., e^{j(\frac{M_1-1}{2})u_l}]^{\mathrm{T}} \tag{15}$$

and

$$\mathbf{c}(v_l) = [e^{-j(\frac{M_2-1}{2})v_l}, ..., e^{-jv_l}, 1, e^{jv_l}, ..., e^{j(\frac{M_2-1}{2})v_l}]^{\mathrm{T}}. \tag{16}$$

They can be transformed into real-valued by using the following simplest matrices,

$$\begin{aligned} \mathbf{Q}_{2m} &= \frac{1}{\sqrt{2}}\begin{bmatrix} \mathbf{I}_m & j\mathbf{I}_m \\ \mathbf{\Pi}_m & -j\mathbf{\Pi}_m \end{bmatrix}, \text{if } M \text{ is even} \\ \mathbf{Q}_{2m+1} &= \frac{1}{\sqrt{2}}\begin{bmatrix} \mathbf{I}_m & \mathbf{0} & j\mathbf{I}_m \\ \mathbf{0}^{\mathrm{T}} & \sqrt{2} & \mathbf{0}^{\mathrm{T}} \\ \mathbf{\Pi}_m & \mathbf{0} & -j\mathbf{\Pi}_m \end{bmatrix}, \text{if } M \text{ is odd} \end{aligned} \tag{17}$$

where $2m = M$ if M is even and $2m + 1 = M$ if M is odd, $\mathbf{I}_m$ and $\mathbf{\Pi}_m$ are the unit matrix and the exchange matrix, respectively. Thus, the real-valued steering vectors are $\mathbf{d}(u_l) = \mathbf{Q}_{M_1}^{\mathrm{H}}\mathbf{c}(u_l)$ and $\mathbf{d}(v_l) = \mathbf{Q}_{M_2}^{\mathrm{H}}\mathbf{c}(v_l)$.

We separate the URA into four sub-arrays, e.g., subarrays 1–4. The array size of sub-arrays 1 and 2 is $(M_1 - 1) \times M_2$, while it is $M_1 \times (M_2 - 1)$ for sub-arrays 3 and 4. Sub-arrays 1 and 2 are the same except for the displacement d_x along x-axis. Likewise, sub-arrays 3 and 4 are displaced by d_y. The relationship between the steering vectors of sub-arrays 1 and 2 can be expressed as

$$e^{ju_l}(\mathbf{J}_1\mathbf{c}(u_l)) = \mathbf{J}_2\mathbf{c}(u_l) \tag{18}$$

where $\mathbf{J}_1 = [\mathbf{I}_{(M_1-1)}\mathbf{0}_{(M_1-1)\times 1}]$ and $\mathbf{J}_2 = [\mathbf{0}_{(M_1-1)\times 1}\mathbf{I}_{(M_1-1)}]$. As specified in [12], the invariance relationship satisfied by $\mathbf{c}(u_l)$ is

$$tan(\frac{u_l}{2})\mathbf{K}_{u1}\mathbf{d}(u_l) = \mathbf{K}_{u2}\mathbf{d}(u_l) \tag{19}$$

where $\mathbf{K}_{u1}$ and $\mathbf{K}_{u1}$ are the real and imaginary parts of $(\mathbf{Q}_{M_1-1}^{\mathrm{H}}\mathbf{J}_2\mathbf{Q}_{M_1})$, respectively.

Further considering L paths, (19) can be written as

$$\mathbf{K}_{u1}\mathbf{D}\mathbf{\Omega}_u = \mathbf{K}_{u2}\mathbf{D} \tag{20}$$

with $\mathbf{D} = [\mathbf{d}(u_1), \mathbf{d}(u_2), ..., \mathbf{d}(u_L)]$ and $\mathbf{\Omega}_u = diag\{tan(\frac{u_1}{2}), ..., tan(\frac{u_L}{2})\}$.

Similarly, we can get

$$\mathbf{K}_{v1}\mathbf{D}\mathbf{\Omega}_u = \mathbf{K}_{v2}\mathbf{D} \tag{21}$$

where $\mathbf{K}_{v1}$ and $\mathbf{K}_{v2}$ are the real and imaginary parts of $(\mathbf{Q}_{M_2-1}^{\mathrm{H}}\mathbf{J}_2\mathbf{Q}_{M_2})$, respectively.

In accordance with the stretched matrix in (5) and performing the real-valued computation, the received signal should be written as $\mathbf{Y}_{vec}(k) = (\mathbf{Q}_{M_1}^{\mathrm{H}} \otimes \mathbf{Q}_{M_2}^{\mathrm{H}})\mathbf{Y}(k)$. Let $\mathbf{E}_s$ being the L "largest" left singular vectors of $[Re\{\mathbf{Y}_{vec}(k)\}, Im\{\mathbf{Y}_{vec}(k)\}]$, it is related to $\mathbf{D}$ with an unknown $L \times L$ real-valued matrix, i.e., $\mathbf{E}_s = \mathbf{DT}$. Then, by substituting $\mathbf{D} = \mathbf{E}_s\mathbf{T}^{-1}$ to (20) and (21) we can get

$$\mathbf{\Psi}_u = (\mathbf{K}_{u1}\mathbf{E}_s)^{-1}\mathbf{K}_{u2}\mathbf{E}_s \tag{22}$$

and

$$\mathbf{\Psi}_v = (\mathbf{K}_{v1}\mathbf{E}_s)^{-1}\mathbf{K}_{v2}\mathbf{E}_s \tag{23}$$

where $\mathbf{\Psi}_{(\cdot)} = \mathbf{T}^{-1}\mathbf{\Omega}_{(\cdot)}\mathbf{T}$. This refers to the joint diagonalization problem which can be solved by computing the eigenvalues $\{\gamma_1, ..., \gamma_L\}$ of $\mathbf{\Psi}_u + j\mathbf{\Psi}_v$. Then, u_l and v_l are given as

$$\begin{aligned} u_l &= 2tan^{-1}(Re\{\gamma_l\}) \\ v_l &= 2tan^{-1}(Im\{\gamma_l\}). \end{aligned} \tag{24}$$

Finally, the AAoA and EAoA can be calculated as follows,

$$\begin{aligned} \phi_l &= tan^{-1}(\frac{v_l}{u_l}) \\ \theta_l &= sin^{-1}(\sqrt{(\frac{\lambda}{2\pi d_x}u_l)^2 + (\frac{\lambda}{2\pi d_y}v_l)^2}). \end{aligned} \tag{25}$$

Through (25), AAoAs are calculated from 0° to 180°, one way to map them into 0° to 360° is observing the positive/negtive signs of u_l and v_l.

Due to the constraints mentioned previously, we know that MUSIC and Unitary ESPRIT algorithms can only work when the path number is smaller than the antenna number in incoherent environment.

C. SAGE Algorithm

SAGE algorithm is an iteratively maximum likelihood estimation method, which can be divided into two steps: expectation (E) and M steps. "E" step is to extract the unobservable data $\mathbf{X}_l(k)$ from the observable data $\mathbf{Y}(k)$ using the initial assumed or previous estimated parameters $\widehat{\Omega}_{l'}^{'} = [\widehat{\phi}_{l'}^{'}, \widehat{\theta}_{l'}^{'}]$ of the $l^{'}$-th path, i.e.,

$$\begin{aligned} \widehat{\mathbf{X}}_l(k; \widehat{\Omega}_l^{'}) &= \mathrm{E}[\mathbf{X}_l(k)|\mathbf{X}(k), \widehat{\Omega}_{l'}^{'}] \\ &= \mathbf{Y}(k) - \sum_{l'=1, l'\neq l}^{L} \mathbf{X}_{l'}(k; \widehat{\Omega}_{l'}^{'}) \end{aligned} \tag{26}$$

Given the extracted data above, parameters of the l-th path can be derived by searching the angles that can maximize the following cost function,

$$\mathbf{z} = \mathbf{c}^{\mathrm{H}}(u_l, v_l)\sum_{k=1}^{K}\widehat{\mathbf{X}}_l(k; \widehat{\Omega}_l^{'}) \tag{27}$$

Then, AAoAs and EAoAs can be searched as follows,

$$\widehat{\phi}_l^{''} = arg\max\{|z(\phi, \widehat{\theta}_l^{'}); \widehat{\mathbf{X}}_l(k; \widehat{\Omega}_l^{'}|)\} \tag{28}$$

$$\widehat{\theta}_l^{''} = arg\max\{|z(\widehat{\phi}_l^{''}, \theta; \widehat{\mathbf{X}}_l(k; \widehat{\Omega}_l^{'}|)\}. \tag{29}$$

This is the "M" step of the SAGE algorithm. Iteratively carrying out the "E" and "M" steps, a sequence of estimates can be generated until the cost function converges to a stationary point.

IV. Simulation and Measurement Analysis

A. Simulation Results

In accordance with the channel measurement setups, the theoretical settings to observe the estimation performance of MUSIC algorithm are shown in Table I. Note that we assume 4 multipaths with EAoAs of the first two MPCs differed by $2°$, and EAoAs of the second and third MPCs are the same. Thus, we can have a simple observation of the performance for MUSIC algorithm to distinguish closely spaced MPCs. The Rx square array number is set to 16 and 64, respectively, to study the impact of antenna number on estimation performance.

Fig. 1 is the simulation results of the MUSIC algorithm. Angles corresponding to the normalized spectrum peaks are the estiamted AAoAs and EAoAs. It can be seen that in Fig. 1(a), there are slight ambiguities around the first three paths. Moreover, there are more than three peaks are formed which will introduce extra false MPCs into the estimation results. When the array number increases to 64, four peaks can be clearly isolated, as shown in Fig. 1(b). By searching the multiple local maxima, the AoAs of four paths can be accurately located in this case.

As shown in Fig. 2, the RMSEs versus SNRs are calculated for the MUSIC and Unitary ESPRIT algorithms to estimate single path using different array numbers, i.e., 2×2 and 4×4. The AAoA and EAoA are set to $50°$ and $62°$, respectively. It is clear to see that the estimation performance of both algorithms can be improved significantly with the increase of SNR and array number. Comparing MUSIC and Unitary ESPRIT algorithms, we can see that when array size is 2×2, Unitary ESPRIT algorithm shows better performance than MUSIC algorithm. However, with the increase of SNR and array size, MUSIC algorithm performs better than Unitary ESPRIT algorithm.

As was studied in many literatures, the SAGE algorithm can provide perfect estimation results even when the SNR and array number is very small. Therefore, the perfect simulation results of SAGE algorithm are not shown in this part.

B. Measurement Results

To study the estimation performance of those three algorithms in real measurement data processing, the channel measurement data acquired in a typical indoor environment using vector network analyzer (VNA) is selected. Relative channel measurement setups are the same with that listed in Table I. The configurations of Tx and Rx array are shown in Fig. 3, it is a typical line-of-sight (LoS) scenario. We can see that the Tx horn antenna is pointed to Rx virtual array center, and the distance between Tx and Rx array center is 2.84 m. The angles between Tx and Rx can be calculated according to the geometry relationship. Note that there is a vertically placed white board, which is right beside the Rx array.

As shown in Fig. 4, the MUSIC algorithm is used to estimate the angles by assuming 50 MPCs. Six obvious clusters with EAoAs range from $50°$ to $90°$ can be found. They are corresponding to the LoS, single bounce, or even double bounces components. The AAoAs and EAoAs can be located by search for the spectrum peaks, as shown in Fig. 5.

In Fig. 5, estimation results using the MUSIC, Unitary ESPRIT, and SAGE algorithms are given. The assumed MPC numbers are 20 and 50 for Unitary ESPRIT and SAGE algorithms, respectively. The reason for assuming 20 paths for Unitary ESPRIT algorithm is that, when the assumed path number is increased, many unreasonable MPCs are extracted by comparing to the real environment setups. This is caused by the poor estimation performance of Unitary ESPRIT algorithm in highly correlated environment. As the spectrum peaks of MUSIC algorithm are exhibit in humps, so we select 300 angles with large normalized spectrum values as estimated parameters. We can see that strong LoS component with AAoA=$180°$ and EAoA=$66°$, and single bounce components with AAoA centering at $0°/360°$ can be estimated by three algorithms. We can see that even though the results are not exactly the same, several clusters are consistent for MUSIC and SAGE algorithms. Thus, we draw conclusion that MUSIC algorithm is applicable in 16 GHz massive MIMO channel

TABLE I
Parameter Settings.

Parameter	Simulation setting
Center frequency, f (GHz)	16
Sample points, K	100
Antenna spacing step, $d_x = d_y$ (mm)	8
Path number, L	4
SNR, ρ	20
AAoA, ϕ ($°$)	$(50, 60, 70, 90)$
EAoA, θ ($°$)	$(62, 60, 60, 50)$
Monte Carlo simulations	500

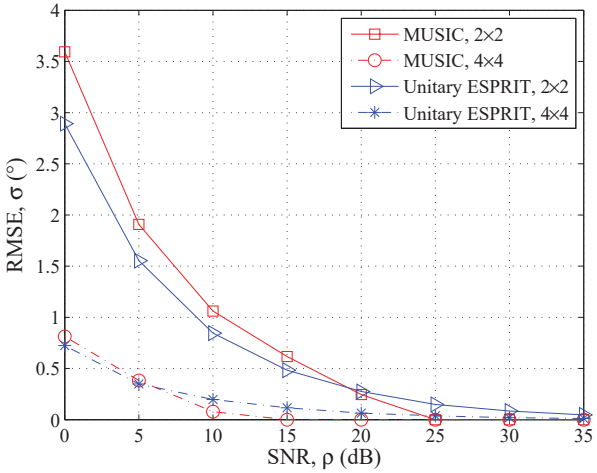

Fig. 2. RMSE comparison of the MUSIC and Unitary ESPRIT algorithms.

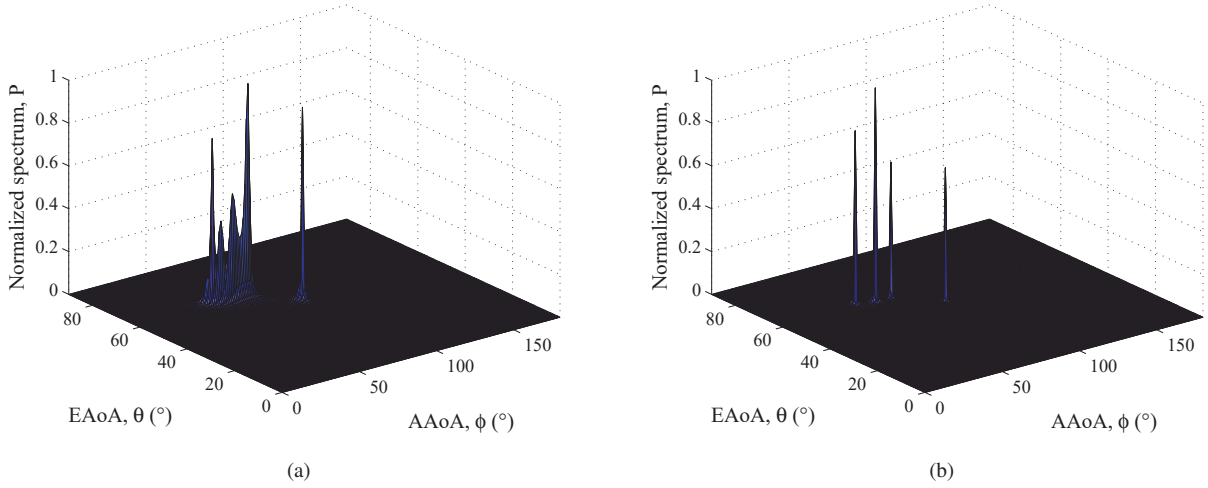

Fig. 1. Normalized spectrums of MUSIC algorithm (a) with M=16 and (b) with M=64.

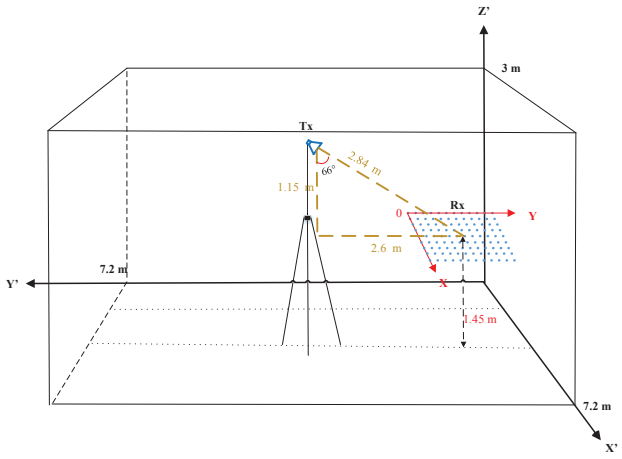

Fig. 3. Configurations of Tx and Rx array.

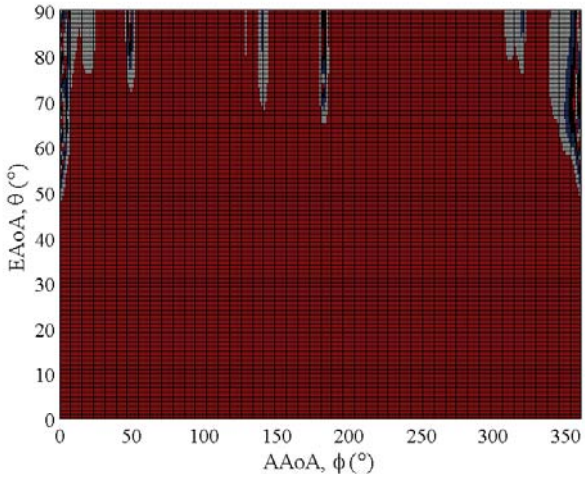

Fig. 4. Measurement data estimation results using the MUSIC algorithm.

measurement data processing.

V. Conclusions

In this paper, we have introduced some basic knowledge about the MUSIC, Unitary ESPRIT, and SAGE algorithms. In terms of the computational complexity, it has been indicated that the SAGE algorithm has to search angles at each iteration step, MUSIC needs to search angles once, whilst Unitary ESPRIT affords to calculate the AoAs directly. To analyze the estimation performance, the impacts of SNR, antenna number, and MPC angle differences on estimation performance have been analyzed for MUSIC and Unitary ESPRIT algorithms. The SAGE algorithm can always provide the highest accuracy than the other two algorithms. It has been shown that the MUSIC algorithm has better performance than the Unitary ESPRIT with large array size and SNR. Three algorithms have been used to estimate AoAs from indoor channel measurement data at 16 GHz. Results have shown that both the MUSIC and Unitary ESPRIT algorithms are able to extract the strong LoS and single bounce components, but the Unitary ESPRIT algorithm perform less satisfied in extracting the rest of MPCs. Comparing the MUSIC algorithm with the SAGE algorithm, it has been shown that the MUSIC algorithm can provide comparable performance with the SAGE algorithm. Thus, considering the tradeoff between complexity and accuracy, we draw conclusion that the MUSIC algorithm is applicable in massive MIMO channel measurement data processing at 16 GHz indoor environment.

Acknowledgment

The authors would like to acknowledge the support from Natural Science Foundation of China (No. 61771293, 61371110), Xinwei Telecom Technology Inc. (Grant No. 11131701), Fundamental Research Funds of Shandong University (No. 2017JC029), Key R&D

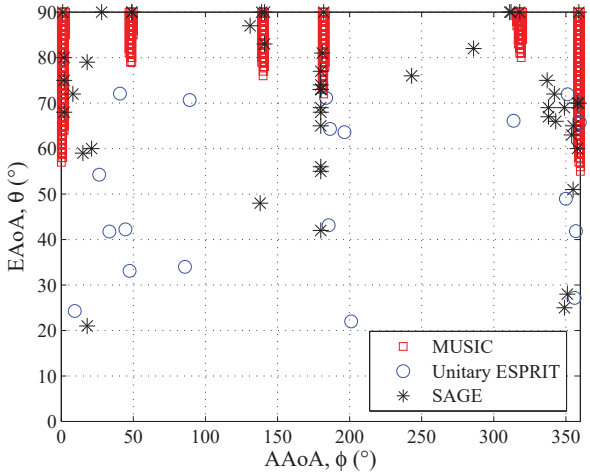

Fig. 5. Estimation results using three algorithms.

Program of Shandong Province (No. 2016GGX101014), EPSRC TOUCAN project (No. EP/L020009/1), and EU H2020 RISE TESTBED project (No. 734325).

REFERENCES

[1] C.-X. Wang, F. Haider, X. Gao, X.-H. You, Y. Yang, D. Yuan, H. Aggoune, H. Haas, S. Fletcher, and E. Hepsaydir, "Cellular architecture and key technologies for 5G wireless communication networks," *IEEE Commun. Mag.*, vol. 52, no. 2, pp. 122–130, Feb. 2014.

[2] B. H. Fleury, M. Tschudin, R. Heddergott, D. Dahlhaus, and K. I. Pedersen, "Channel parameter estimation in mobile radio environments using the SAGE algorithm," *IEEE J. Sel. Areas Commun.*, vol. 17, no. 3, pp. 434–450, Mar. 1999.

[3] H. Krim and M. Viberg, "Two decades of array signal processing research: the parametric approach," *IEEE Sig. Proc. Mag.*, vol. 13, no. 4, pp. 67–94, Jul. 1996.

[4] R. O. Schmidt, "Multiple emitter location and signal parameter estimation," *IEEE Trans. Antennas Propag.*, vol. AP-34, no. 3, pp. 276–280, Mar. 1986.

[5] R. Roy, A. Paulraj, and T. Kailath, "ESPRIT–A subspace rotation approach to estimation of parameters of cisoids in noise," *IEEE Trans. ASSP*, vol. 34, no. 5, pp. 1340–1342, Oct. 1986.

[6] R. Roy and T. Kailath, "ESPRIT-estimation of signal parameters via rotational invariance techniques," *IEEE Trans. ASSP*, vol. 37, no. 7, pp. 984–995, Jul. 1989.

[7] M. Haardt and J. A. Nossek, "Unitary esprit: how to obtain increased estimation accuracy with a reduced computational burden," *IEEE Trans. Sig. Proc.*, vol. 43, no. 5, pp. 1232–1242, May 1995.

[8] M. Feder and E. Weinstein, "Parameter estimation of superimposed signals using the EM algorithm," *IEEE Trans. ASSP*, vol. 36, no. 4, pp. 477–489, Apr. 1988.

[9] B. H. Fleury, D. Dahlhaus, R. Heddergott, and M. Tschudin, "Wideband angle of arrival estimation using the SAGE algorithm," in *Proc. IEEE ISSSTA'96*, Mainz, Sep. 1996, pp. 79–85.

[10] X. F. Yin, L. X. Ouyang, and H. W. Wang, "Performance comparison of SAGE and MUSIC for channel estimation in direction-scan measurements," *IEEE Access*, vol. 4, no. 1, pp. 1163–1174, Mar. 2016.

[11] T. Wang, B. Ai, R. S. He, and Z. D. Zhong, "Two-dimension direction-of-arrival estimation for massive MIMO systems," *IEEE Access*, vol. 3, no. 1, pp. 2122–2128, Nov. 2015.

[12] M. D. Zoltowski, M. Haardt, and C. P. Mathews, "Closed-form 2-D angle estimation with rectangular arrays in element space or beamspace via unitary ESPRIT," *IEEE Trans. Sig. Proc.*, vol. 44, no. 2, pp. 316–328, Feb. 1996.